International Journal of Non-Linear Mechanics ▮ (▮▮▮▮) ▮▮▮–▮▮▮

Contents lists available at ScienceDirect

International Journal of Non-Linear Mechanics

journal homepage: www.elsevier.com/locate/nlm

Discontinuous synchrony in an array of Van der Pol oscillators

Przemyslaw Perlikowski [a,b], Andrzej Stefanski [a,*], Tomasz Kapitaniak [a]

[a] Division of Dynamics, Technical University of Lodz, Stefanowskiego 1/15, 90-924 Lodz, Poland
[b] Institute of Mathematics, Humboldt University of Berlin, Unter den Linden 6, 10099 Berlin, Germany

ARTICLE INFO

Article history:
Received 24 November 2008
Received in revised form
27 November 2009
Accepted 28 January 2010

Keywords:
Complete synchronization
Van der Pol oscillator
Ragged synchronizability
Clusters

ABSTRACT

We show the phenomenon of complete synchronization in an network of coupled oscillators. We confirm that non-diagonal coupling can lead to the appearance or disappearance of synchronous windows (ragged synchronizability phenomenon) in the coupling parameter space. We also show the appearance of clusters (synchronization in one or more group) between coupled systems. Our numerical studies are confirmed by an electronic experiment.

1. Introduction

Collective dynamics of coupled systems has been known for a long time, i.e., since the second half of 17th century, when Huygens discovered the synchronization of two clock pendulums [10]. Next, this phenomenon has been observed and investigated in various types of mechanical or electrical systems [5,19,24]. Recently, the idea of synchronization has been also adopted for chaotic systems [15] and it has become an object of great interest in many areas of science, e.g., biology [9,22], communication [6] or laser physics [28,32].

Through the last years a number of new types of synchronization have been identified [20,21] and new interesting ideas have appeared [3,27]. It has been demonstrated that two or more chaotic systems can synchronize if they are under control of some connection mechanisms. Typical examples of such mechanisms are drive-response [15,16] or active-passive decomposition [13] of the considered system, direct bi-directional (mutual) or unidirectional (master-slave) diffusive coupling between the oscillators [12,29,30].

In our previous work [23], we presented an example of non-diagonally coupled array of Duffing oscillators, in which multiple disconnected synchronous regions of coupling strength occur. The term non-diagonal coupling means that the network nodes are linked with others via non-diagonal components of linking (output) function. We have also observed the appearance or disappearance of such synchronous windows in coupling parameter space, when the number of oscillators in the array or topology of connections between them changes. This phenomenon has been called the ragged synchronizability (RSA). The existence of the RSA has been confirmed numerically [23] and experimentally [17]. Usually, in papers concerning these new ideas classical autonomous dynamical systems have been used as the examples, i.e., the Lorenz and Rössler oscillators, non-linear discrete-time systems (e.g. logistic and Henon map), neuron models etc. On the other hand there is a lack of works on new synchronization concepts applied for non-autonomous systems like mechanical or electrical oscillators with external forcing. Hence, this paper deals with synchronization of non-linear oscillators with a harmonic driving (Section 5), where phenomena of the RSA and clustering (synchronization of oscillator's subgroups) can be observed. For needs of clear presentation of the RSA effect we concentrated on the complete synchronization (CS) mode in sense of total time-coincidence of phases and amplitudes. The synchronization of periodic responses with phase shift is represented here by effect of clustering. In the numerical analysis, the Van der Pol (VdP) [26] oscillator with non-linear damping, which can be treated as an equivalent of mechanical self-excited system, has been applied as an array node system. Such a choice is due to option of continuous control of the system parameters in electrical oscillators. Then the experimental bifurcational analysis of the system dynamics is possible.

This paper is organized as follows. In Section 2 basic definitions concerning synchronization problems under consideration are presented. Section 3 approaches the idea of Master Stability Function (MSF) [14], which is a main tool for carried out analysis of the synchronization. Next Section 4 contains an detailed description of investigated VdP oscillator. Results of

* Corresponding author.
E-mail address: steve@p.lodz.pl (A. Stefanski).

0020-7462/$ - see front matter © 2010 Elsevier Ltd. All rights reserved.
doi:10.1016/j.ijnonlinmec.2010.01.010

numerical and experimental study and their comparison are demonstrated in Section 5. The paper finishes with conclusions (Section 6).

2. Synchronization and clustering

Pecora and Carroll [15] defined the CS between two dynamical systems as a state when their state trajectories $x(t)$ and $y(t)$ converge to the same values and continue in such relation further in time. Thus, the CS means a full coincidence of phases (frequencies) and amplitudes of the systems response. Earlier the problem of the CS threshold in arrays of coupled identical oscillators was studied by Fujisaka and Yamada [8,30] and Pikovsky [18].

Definition 1.1. Complete synchronization of two dynamical systems represented with their phase plane trajectories $x(t)$ and $y(t)$, respectively, takes place when the following relation is fulfilled:

$$\lim_{t\to\infty}\|\mathbf{x}(t)-\mathbf{y}(t)\|=0. \tag{1}$$

It is also described in the subject literature as identical or full synchronization [16,20]. The CS state can be reached only when two identical dynamical systems are concerned, say, they are given with the same ODEs with identical system parameters. This condition of identity may not be fulfilled due to presence of an external noise or parameters mismatch what usually can happen in real systems. If scale of such disturbances is relatively small, then both systems may eventually reach a state called imperfect complete synchronization (ICS) [12], sometimes named as practical or disturbed synchronization.

Definition 1.2. Imperfect complete synchronization of two dynamical systems represented with their phase plane trajectories $x(t)$ and $y(t)$, respectively, occurs when the following inequality is fulfilled

$$\lim_{t\to\infty}\|\mathbf{x}(t)-\mathbf{y}(t)\|\le\varepsilon, \tag{2}$$

where ε is a small parameter. The CS (or the ICS) of entire network or array of mechanical oscillators means a collective motion of them, i.e., they have the same position and velocity in each moment of time evolution. However, if there is a set composed of $N>2$ identical nodes then it can be divided into two or more subsets within which the motion of oscillators is collective while between subsets the dynamics is uncorrelated or at least a phase shift is observed, e.g. two groups of subsystems in anti-phase regime. Such subgroups of synchronized oscillators are called clusters [4,11].

3. Stability of synchronous state

Consider a dynamical system

$$\dot{\mathbf{x}}=\mathbf{f}(\mathbf{x}), \tag{3}$$

where $x\in\mathbb{R}^m$.

The dynamics of any network of N identical oscillators can be described in block form:

$$\dot{\mathbf{x}}=\mathbf{F}(\mathbf{x})+(\sigma\mathbf{G}\otimes\mathbf{H})\mathbf{x}, \tag{4}$$

where $\mathbf{x}=(\mathbf{x}_1,\ldots,\mathbf{x}_N)$, $\mathbf{F}(\mathbf{x})=(\mathbf{f}(\mathbf{x}_1),\ldots,\mathbf{f}(\mathbf{x}_N))$, $\mathbf{G}$ is the connectivity matrix, i.e., the Laplacian matrix representing the topology of connections between the network nodes, σ is the overall coupling coefficient, $\otimes$ is a direct (Kronecker) product of two matrices and $\mathbf{H}:\mathbb{R}^m\to\mathbb{R}^m$ is an output function of each oscillator's variables that is used in the coupling (it is the same for all nodes).

After the derivation the variational equation of the network system (4) is as follows

$$\dot{\boldsymbol{\xi}}=[\mathbf{I}\otimes D\mathbf{F}+\sigma(\mathbf{G}\otimes D\mathbf{H})]\xi, \tag{5}$$

where $\boldsymbol{\xi}=(\xi_1,\xi_2,\ldots,\xi_N)$ represents collection of perturbation, $\mathbf{I}$ is an identity matrix and $D\mathbf{F}$, $D\mathbf{H}$ are Jacobi matrices of system (4) and output function, respectively.

After the block diagonalization of the variational equation (Eq. (5)) we have

$$\dot{\xi}_k=[D\mathbf{f}+\sigma\gamma_k D\mathbf{H}]\xi_k, \tag{6}$$

For $\gamma_0=0$ we have linearized the equation of the node system (Eq. (3)) which is corresponding to the mode longitudinal to invariant synchronization manifold $\mathbf{x}_1=\mathbf{x}_2=\cdots=\mathbf{x}_N$. The remaining $N-1$ eigenvalues represent different transverse modes of perturbation from synchronous state. In the general case they can be complex numbers. However, for identical coupled mechanical oscillators eigenvalues γ_k are real numbers due to the symmetry of coupling. This symmetry results from a mutual character of the interaction between mechanical systems according to 3rd Newton's law of dynamics. Such a symmetry of coupling (i.e. diagonal symmetry of connectivity matrix $\mathbf{G}$) results from the identity of coupled oscillators. In case of non-identical systems (e.g. different masses of the oscillators) there appear non-symmetry in matrix $\mathbf{G}$, in spite of mutual interaction of oscillators.

Assuming that γ represents an arbitrary value of γ_k and ζ symbolizes an arbitrary transverse mode ξ_k, we can define the generic variational equation for any node system

$$\dot{\zeta}=[D\mathbf{f}+\sigma\gamma D\mathbf{H}]\zeta. \tag{7}$$

Generic variational equation (Eq. (7)) describes an evolution of any perturbation in the directions transversal to the final synchronous state, that dynamics is governed by Eq. (3). Now, we can obtain the MSF for the considered case as the largest transversal Lyapunov exponent λ_T^1, calculated for generic variational equation (Eq. (7)), including the solution of Eq. (3), in function of the product $\sigma\gamma$. An exemplary MSF graph is depicted in Figs. 1a and b. If discrete spectrum of products $\sigma\gamma_k$ corresponding to all transversal eigenmodes can be found in the ranges of negative transversal Lyapunov exponent (see Fig. 1a) then synchronous state is stable for the analyzed configuration of couplings. This is a necessary condition for synchronization of all network nodes. However, sometimes it may not be a sufficient one due to possible local instability of the synchronization manifold [2]. On the other hand, if even one of values $\sigma\gamma_k$ is located in the range of positive λ_T^1 (see Fig. 1b) then the CS of all oscillators is impossible, but synchronization in clusters can occur.

4. Analyzed oscillator

A graphical representation of the analyzed mechanical oscillator is shown in Fig. 2a. This is a well known Van der Pol (VdP) oscillator with non-linear damping $d(1-y^2)$ and linear spring characteristic k_y which can be considered as an equivalent of self-excited mechanical oscillator. We apply additional harmonic driving of VdP circuits for needs of experiment because the signal from common external generator allowed us to easy control of the circuits dynamics and improved the identity of array systems during the experimental research.

Assuming, under harmonic driving with amplitude A the system under consideration can be described by the following

Please cite this article as: P. Perlikowski, et al., Discontinuous synchrony in an array of Van der Pol oscillators, Int. J. Non-Linear Mech. (2010), doi:10.1016/j.ijnonlinmec.2010.01.010

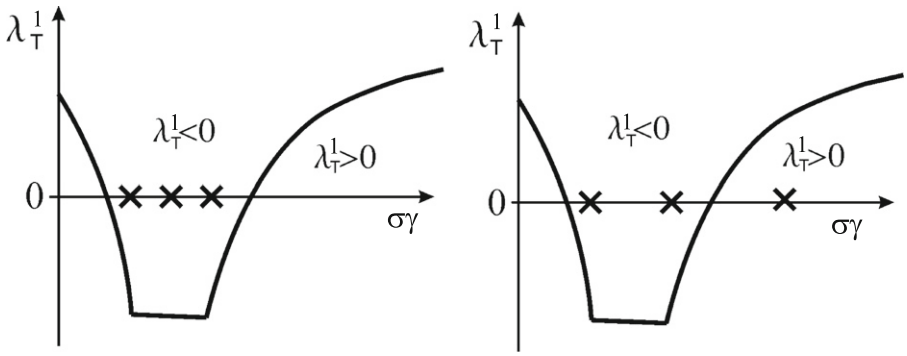

Fig. 1. Examples of the MSFs.

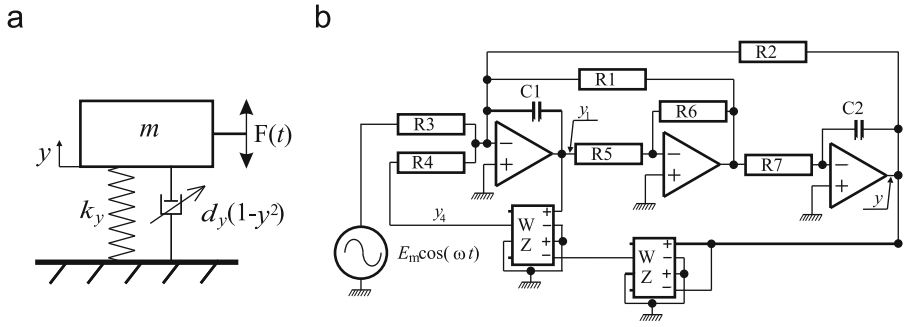

Fig. 2. Scheme of single VdP oscillator: (a) mechanical and (b) electrical.

second order differential equation

$$m\ddot{y} = d_y(1-y^2)\dot{y} - k_y y + A\cos(\Omega t), \tag{8}$$

where Ω represents the frequency of the external excitation ($F(t) = A\cos(\Omega t)$).

During experimental studies we have used the classical electrical version of VdP oscillator [26,25] which allowed us to detailed bifurcational analysis of the researched problem.

A scheme of applied electrical circuit is shown in Fig. 2b. The circuit is composed of two capacitors $C1$ and $C2$, seven resistors $R(1-7)$ and two multiplicators AD-633JN [1] which introduce non-linearity. Multiplicators have the following characteristic $W = (1/V_c)(X_1 - X_2)(Y_1 - Y_2) + Z$, where X_1, X_2, Y_1 and Y_2 are the input signals, W is an output signal, Z is a correction to output signal and $V_c = 10\,\mathrm{V}$ is a characteristic voltage. The error caused by multiplicator is less the 2% and the input resistance is 10 MΩ and has negligible influence on input signal.

Oscillator is supplied by direct 18 V current from amplifier ZPA 81. The forcing signal $E_m\cos(\omega t)$ is generated in generator G 432 with maximum amplitude $E_m = 5\,\mathrm{V}$ and frequency in range $\omega \in (0\,\mathrm{Hz}, 1\,\mathrm{MHz})$. The additional resistors $R8$ and R have been used to realize the coupling.

The node system y_1 is given by equation:

$$y_1 = \frac{1}{C1R4}\int y_4\,\mathrm{d}t - \frac{1}{R2C1}\int y\,\mathrm{d}t - \frac{1}{R1C1}\int\left(-\frac{R6}{R5}y_1\right)\mathrm{d}t + -\frac{1}{R3C1}\int E_m\cos(\omega t)\,\mathrm{d}t. \tag{9}$$

Basis on multiplicator property one can write

$$y_4 = \frac{y_1 y^2}{100\,\mathrm{V}^2}. \tag{10}$$

Signal y is given by formula:

$$y = -\frac{1}{R7C2}\int\left(-\frac{R6}{R5}y_1\right)\mathrm{d}t = \frac{R6}{R5R7C2}. \tag{11}$$

After derivation of Eq. (11):

$$\dot{y} = \frac{R6}{R5R7C2}y_1, \tag{12}$$

and rearranging of Eq. (12) one can determinate y_1:

$$y_1 = \frac{R5R7C2}{R6}\dot{y}. \tag{13}$$

Substitute Eq. (9) to (12):

$$\dot{y} = \frac{R6}{R5R7C2}\left(\frac{1}{C1R4}\int y_4\,\mathrm{d}t - \frac{1}{R2C1}\int y\,\mathrm{d}t - \frac{1}{R1C1}\int\left(-\frac{R6}{R5}y_1\right)\mathrm{d}t + -\frac{1}{R3C1}\int E_m\cos(\omega t)\,\mathrm{d}t\right). \tag{14}$$

After derivation Eq. (14) has following form:

$$\ddot{y} = \frac{R6}{R5R7C2}\left(\frac{1}{C1R4}y_4 - \frac{1}{R2C1}y - \frac{1}{R1C1}\left(-\frac{R6}{R5}y_1\right) + -\frac{1}{R3C1}E_m\cos(\omega t)\right). \tag{15}$$

Substitute Eqs. (10) and (13) to Eq. (15), and use dependence $100R4 \approx R1$ one can achieve

$$\ddot{y} - \frac{1}{C1R1}(1-y^2)\dot{y} + \frac{1}{C1C2R2R7}y = \frac{E_m\cos(\omega t)}{C1C2R3R7}. \tag{16}$$

For numerical analyse it is necessary to rewrite Eq. (16) in two dimensionless first order equations

$$\dot{z} = x,\quad \dot{x} = d(1-x^2)z - x + \cos(\Omega\tau), \tag{17}$$

where $\omega_0^2 = 1/C1C2R2R7$, $d = 1/C1R1\omega_0$, $\Omega = \omega/\omega_0$, $x = yR3/E_mR2$, $\dot{x} = \dot{y}R3/E_mR2\omega_0$, $\ddot{x} = \ddot{y}R3/E_mR2\omega_0^2$.

5. Numerical and experimental results

In the experiment an array of three VdP-type oscillators coupled via linear springs of a rate k, shown in Fig. 3a, was investigated. The evolution of each oscillator coupled in array is

Please cite this article as: P. Perlikowski, et al., Discontinuous synchrony in an array of Van der Pol oscillators, Int. J. Non-Linear Mech. (2010), doi:10.1016/j.ijnonlinmec.2010.01.010

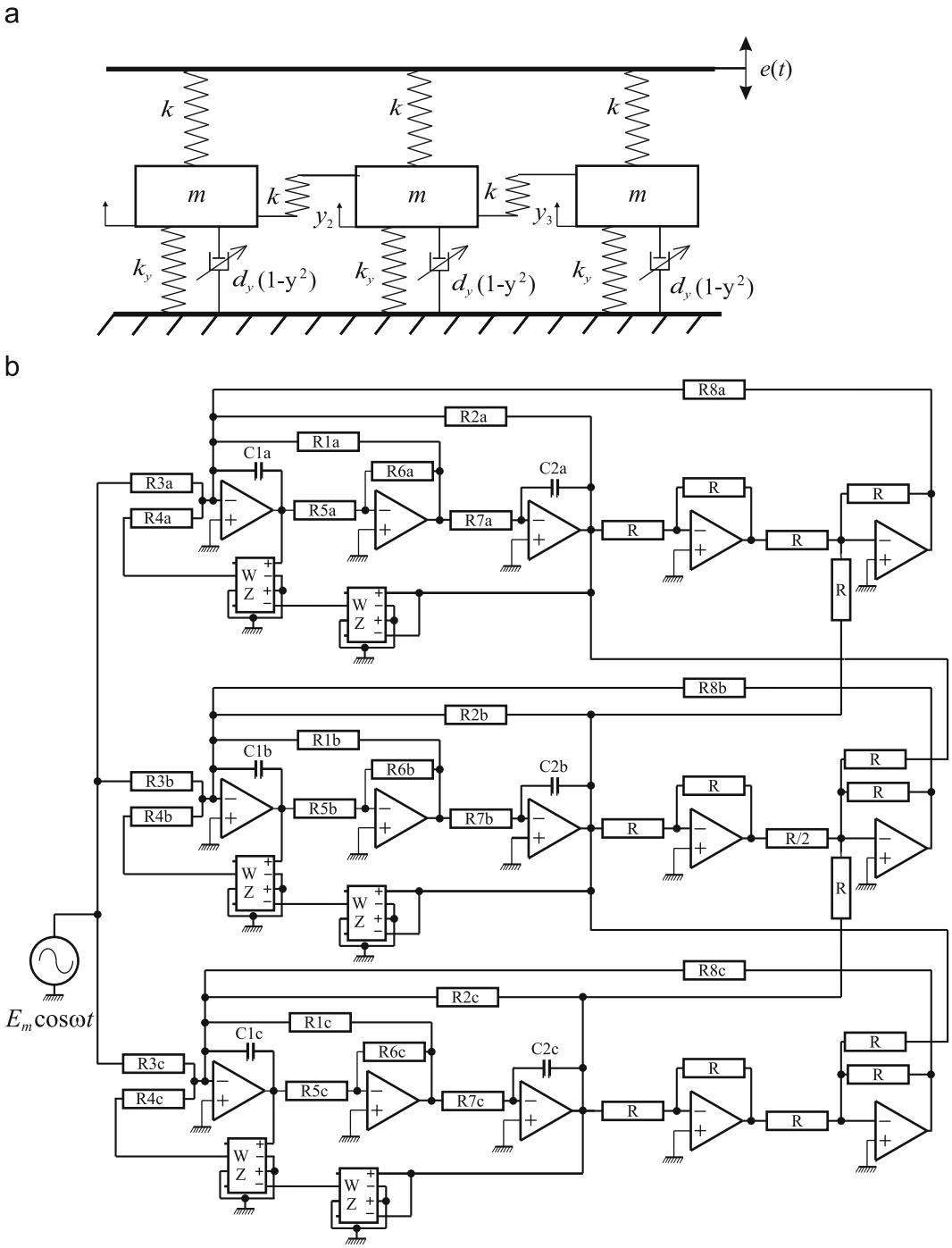

Fig. 3. The model of an open array of Van der Pol's oscillators in a mechanical (a) and electrical (b) representation.

given by the following set of dimensionless equations:

$$\dot{x}_1 = z_1, \tag{18a}$$

$$\dot{z}_1 = d(1-x_1^2)z_1 - x_1 + \cos(\Omega\tau) + \sigma(x_2 - x_1), \tag{18b}$$

$$\dot{x}_2 = z_2, \tag{18c}$$

$$\dot{z}_2 = d(1-x_2^2)z_2 - x_2 + \cos(\Omega\tau) + \sigma(x_1 + x_3 - 2x_2), \tag{18d}$$

$$\dot{x}_3 = z_3, \tag{18e}$$

$$\dot{z}_3 = d(1-x_3^2)z_3 - x_3 + \cos(\Omega\tau) + \sigma(x_2 - x_3), \tag{18f}$$

where $\sigma = R2/R8$ is a constant coupling coefficient.

In the numerical analysis we assumed $d = 0.401$, resulting from real parameters of experimental circuit, and considered Ω and σ as control parameters. The coupling via springs can be classified as the case of pure (diagonal components are equal to zero) ND coupling due to the form of output function

$$\mathbf{H} = \begin{bmatrix} 0 & 0 \\ 1 & 0 \end{bmatrix}. \tag{19}$$

The structure of the nearest-neighbor connections of array nodes is described by the following connectivity

Please cite this article as: P. Perlikowski, et al., Discontinuous synchrony in an array of Van der Pol oscillators, Int. J. Non-Linear Mech. (2010), doi:10.1016/j.ijnonlinmec.2010.01.010

matrix

$$\mathbf{G}=\begin{bmatrix}-1 & 1 & 0\\ 1 & -2 & 1\\ 0 & 1 & -1\end{bmatrix}. \tag{20}$$

Matrix **G** has the following eigenvalues $\gamma_0=0$, $\gamma_1=-1$, $\gamma_2=-3$. Substituting the analyzed system (Eqs. (17) and (19)) in Eq. (7) we obtain the generic variational equation for calculating the MSF, i.e., $\lambda_T^1(\sigma\gamma)$ in the form

$$\dot{\zeta}=\psi, \tag{21a}$$

$$\dot{\psi}=d(1-x^2)\zeta-2\,\mathrm{d}x\psi\zeta-\psi+\sigma\gamma\psi. \tag{21b}$$

In Fig. 4 desynchronous regions, quantified by the synchronization error

$$e=\sum_{i=2}^{3}\sqrt{(x_1-x_i)^2+(z_1-z_i)^2}, \tag{22}$$

where $i=2,3$, versus the coupling coefficient σ and the frequency of external excitation Ω are depicted.

We assumed that systems are synchronized when value synchronization error e is lower the two percent of its maximum value (here $e_{\max}\approx 1$). Hence, according to such a criterion in the white region $e<0.02$ so the systems are synchronized. On the other hand, grey and black regions denote desynchronization connected with the modes associated with eigenvalues γ_1 and γ_2 respectively. The calculations have been performed according to an idea of the MSF for the probe of two oscillators [7]. One can expect the RSA to appear for $\Omega\in(1.2,1.5)$.

For researched value $\Omega=1.22$ in the absence of coupling each oscillator shows periodic behavior with the period equal to the period of excitation. To obtain better accuracy, in this single case, we calculate the MSF by means of maximum transversal Lyapunov exponent λ_T^1 versus $\sigma\gamma$. In Fig. 5 we present the graphical illustration how the MSF idea can be used to determine the synchronization and desynchronization thresholds. We show that transforming the MSF plot (Fig. 5a) via eigenvalues of connectivity matrix **G** (Fig. 5b) one can determine these ranges for real coupling coefficient σ (Figs. 5c and d). This picture also allows us to clearly present the mechanism of the RSA.

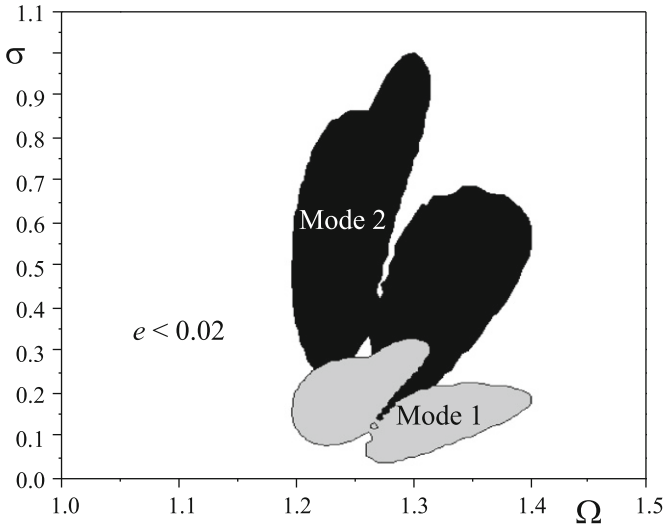

Fig. 4. The synchronization error $e=\sum_{i=2}^{3}\sqrt{(x_1-x_i)^2+(z_1-z_i)^2}$ versus coupling coefficient σ and the frequency of external excitation Ω for Eq. (9); $d=0.401$.

In Fig. 5a one can see the MSF, i.e., the plot of the largest transversal Lyapunov exponent λ_T^1 versus the product $\sigma\gamma$, then in Fig. 5b the lines which correspond to eigenvalues of connectivity matrix **G** (see Eq. (20)) and in Fig. 5c the synchronization error e calculated numerically is presented. Moreover, in Fig. 5d the experimental measurements of the synchronization error e is showed. It is easy to see that synchronization ranges obtained by transformation of the MSF plot via eigenvalues γ_1 and γ_2 (see Fig. 5b) correspond to thresholds determined by numerical (Fig. 5c) and experimental (Fig. 5d) estimation of the synchronization error. In both these diagrams the RSA is visible as the 'windows' of synchronization and desynchronization before the final stable synchronous state is achieved for the coupling strength $\sigma=0.8$. In Fig. 5e we show the zoom with more measurement points of middle synchronized range $(\sigma_{1+}^2,\sigma_{1-}^1)$. The new desynchronized ranges are signed after the index of eigenvalue which cause their appearance (see Figs. 5b, c). Such a notation brings an information which mode (1st or 2nd) desynchronizing bifurcation (superscript) takes place during the transition from the synchronous to the desynchronous regime and which edge of desynchronous interval of the MSF from Fig. 5a (1− and 1+ in subscript correspond to lower and higher edges, respectively) is associated with the given boundary value of the coupling coefficient.

Now let us concentrate on numerical results (Figs. 5a–c) and present in detail the mechanism of creation of the RSA. The CS takes place in the σ−ranges where e approaches zero value. In Fig. 5a one can see one desynchronization range $(1-,1+)$ of the MSF, where the TLE is positive, and on both sides of it two synchronization ranges of the negative TLE, i.e., $\sigma\gamma\in(0,1-)$ and $\sigma\gamma>1+$. However, in Fig. 5c two desynchronous ranges $(\sigma_{1-}^2,\sigma_{1+}^2)$ and $(\sigma_{1-}^1,\sigma_{1+}^1)$ appear, which are separated by narrow synchronization range $(\sigma_{1+}^2,\sigma_{1-}^1)$. First desynchronous interval appears because the mode 1 (associated with eigenvalue γ_1) crosses the desynchronous MSF-interval $(1-,\ 1+)$ while the mode 2 (associated with γ_2) is located in the second synchronous MSF-interval $(1+,\infty)$—see Fig. 5(b). Second desynchronous range is created in the same way. Then in very narrow range $(\sigma_{1+}^2,\sigma_{1-}^1)$ two modes are in synchronous MSF-interval so one can observe "additional middle window" of synchronization in σ−interval. Finally, the steady synchronous state is achieved due to increasing coupling strength at $\sigma=0.8$.

It should be mentioned here that in the experiments it is impossible to avoid parameter mismatches so the complete synchronization is replaced by the ICS in which synchronization error is sufficiently small but not equal to zero. One can see a good agreement in both results. We have estimated a slight disparity of the values of d in all three VdP oscillators with measuring their real parameters. Next, such an approximated mismatch has been realized in the considered model (Eqs. (18a–f)) (the values of d taken in Eqs. 18(b), 18(d) and 18(f) are respectively 0.400, 0.401 and 0.402). The synchronization error simulated numerically for this model is represented with grey line in Fig. 5d. Its good visible agreement with experimental result shows that a slight difference of coupled oscillators does not destroy their synchronization tendency, i.e., the ICS takes place.

In considered network one can also observe the phenomenon of clustering, mentioned above [4,11]. In our case we can obviously observe only (2,1) cluster, i.e, two nodes have common behaviour and one node is independent. We defined the synchronization errors between first and second $(e_{1-2}=\sqrt{(x_1-x_2)^2+(z_1-z_2)^2})$ and first and third $(e_{1-3}=\sqrt{(x_1-x_3)^2+(z_1-z_3)^2})$ oscillator. In Fig. 6 we present results of numerical calculation of synchronization error e_{1-2} (black line) and e_{1-3} (grey line).

Please cite this article as: P. Perlikowski, et al., Discontinuous synchrony in an array of Van der Pol oscillators, Int. J. Non-Linear Mech. (2010), doi:10.1016/j.ijnonlinmec.2010.01.010

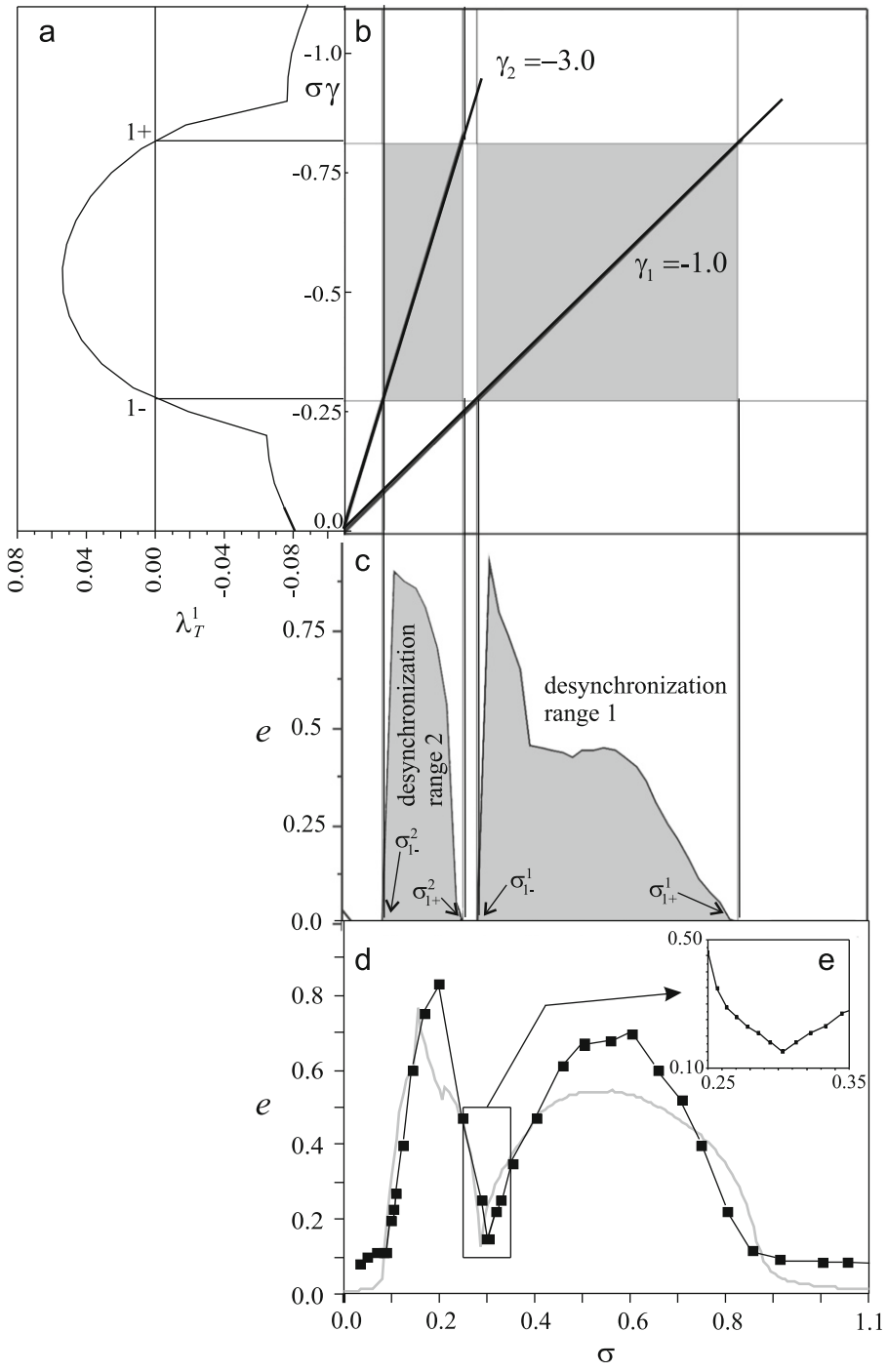

Fig. 5. Projection from the MSF $\lambda_T^1(\sigma\gamma)$ (a) via eigenvalues of the connectivity matrix (b) to the bifurcation diagram of the synchronization error (c) calculated according to Eq. (22). Desynchronization intervals connected with eigenvalues γ_1 and γ_2 are shown in grey; $d=0.401$, $\Omega=1.22$. Comparative diagram of the synchronization error detected experimentally (in black) and numerically with introduced parameter's mismatch (in grey) (d) and its enlargement (e).

As it easy to see in range $\sigma=(0.1,0.27)$ one can observed a cluster between first and third oscillator, while second system is in the desynchronized state with them. This phenomenon is confirmed by calculation of eigenvectors [31] of connectivity matrix **G**. The synchronization in range $\sigma=(0.1,0.27)$ is governed by eigenvalue $\gamma_2=-3.0$ with corresponding eigenvector $v_2=[-0.4082,0.8165,-0.4082]^T$, where first and third component corresponding to synchronized oscillators are identical. Such an equality of two components of v_2 leads to the existence of cluster shown in Fig. 6. The eigenvector of $\gamma_1=-1.0$ is $v_1=[-0.7071,0.0,0.7071]^T$ and clusters do not exists because all components are different.

6. Conclusions

To summarize, we have confirmed and explained the phenomenon of the RSA in the networks of VdP oscillators. Additionally, we have analyzed the process of clustering in considered system. We have shown the mechanism responsible for the appearance or

Please cite this article as: P. Perlikowski, et al., Discontinuous synchrony in an array of Van der Pol oscillators, Int. J. Non-Linear Mech. (2010), doi:10.1016/j.ijnonlinmec.2010.01.010

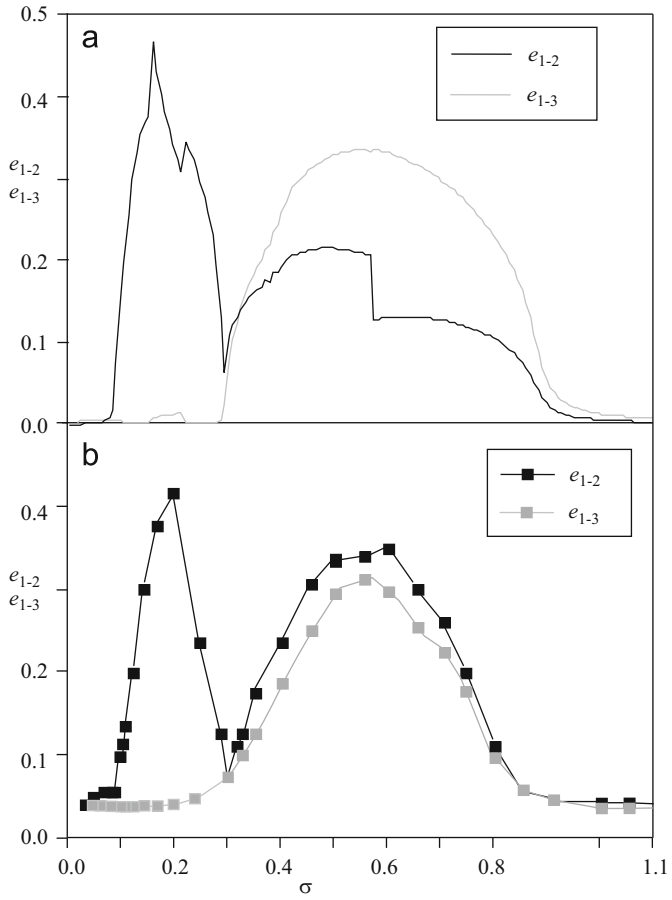

Fig. 6. Comparison of numerical (a) and experimental (b) synchronization error e_{1-2} (black line) and e_{1-3} (grey line) versus coupling coefficient σ; $d=0.401$, $\Omega=1.22$.

disappearance of the windows of synchronizability is the same as the previously studied network of Duffing oscillators [23]. It seems that the phenomena of the RSA and clustering are common for the mechanical systems coupled via elastic element (spring). These effects are also insensitive for the small parameter mismatch, i.e., they can be observed in real mechanical and electrical systems.

Acknowledgments

P.P. acknowledge the support of DFG Research Center Matheon "Mathematics for key technologies" under the project D21. P.P., A.S. and T.K. acknowledge the support of DAAD cooperation under Project No. D0700430, and Department of International Co-operation of Poland under Project DWM/N97/DAAD/2008. A.S. and T.K. acknowledge the support of Polish Department for Scientific Research (DBN) under project No. N N 501 0710 33.

References

[1] Analog Devices, Inc. Low Cost Analog Multiplier, 2002.
[2] P. Ashwin, J. Buescu, I. Stewart, Bubbling of attractors and synchronisation of chaotic oscillators, Phys. Lett. A 193 (2) (1994) 126–139.
[3] A.-L. Barabási, R. Albert, Emergence of scaling in random networks, Science 286 (1999) 509.
[4] V.N. Belykh, I.V. Belykh, E. Mosekilde, Cluster synchronization modes in an ensemble of coupled chaotic oscillators, Phys. Rev. E 63 (3) (2001) 036216.
[5] I.I. Blekman, Synchronization in Science and Technology, ASME Press, New York, 1988.
[6] K.M. Cuomo, A.V. Oppenheim, S.H. Strogatz, Robustness and signal recovery in a synchronized chaotic system, Int. J. Bifurcation Chaos (IJBC) 3 (1993) 1629–1638.
[7] K.S. Fink, G. Johnson, T. Carroll, D. Mar, L. Pecora, Three coupled oscillators as a universal probe of synchronization stability in coupled oscillator arrays, Phys. Rev. E 61 (5) (2000).
[8] H. Fujisaka, T. Yamada, Stability theory of synchronized motion in coupled-oscillator systems, Prog. Theor. Phys. 69 (1983).
[9] J. Hertz, A. Krogh, R. Palmer, Introduction to the Theory of Neural Computation, Addison-Wesley, Reading, MA, 1991.
[10] C. Huygens, Horoloquim Oscilatorium, Pary, 1673.
[11] K. Kaneko, Clustering, coding, switching, hierarchical ordering, and control in network of chaotic elements, Physica D 41 (1990) 137–172.
[12] T. Kapitaniak, M. Sekieta, M. Ogorzalek, Monotone synchronization of chaos, Int. J. Bifurcation Chaos 6 (1996) 211–215.
[13] L. Kocarev, U. Parlitz, Generalized synchronization, predictability, and equivalence of unidirectionally coupled dynamical systems, Phys. Rev. Lett. 76 (11) (1996) 1816–1819.
[14] L. Pecora, Synchronization conditions and desynchronizing patterns in coupled limit-cycle and chaotic systems, Phys. Rev. E 58 (1998).
[15] L. Pecora, T. Carroll, Synchronization of chaotic systems, Phys. Rev Lett 64 (1990).
[16] L. Pecora, T. Carroll, Driving systems with chaotic signal, Phys. Rev. A 44 (1991) 2374.
[17] P. Perlikowski, B. Jagiello, A. Stefaski, T. Kapitaniak, Experimental observation of ragged synchronizability, Phys. Rev. E 78 (2008).
[18] A. Pikovsky, On the interaction of strange attractors, Zeitschrift Phys. B 55 (1984) 149.
[19] J. Rayleigh, Theory of Sound, Dover Publishing, New York, 1945.
[20] M. Rosenblum, A. Pikovsky, J. Kurths, Phase synchronization of chaotic oscillators, Phys. Rev. Lett. 76 (1996) 1804.
[21] N.F. Rulkov, M.M. Sushchik, L.S. Tsimring, H.D.I. Abarbanel, Generalized synchronization of chaos in directionally coupled chaotic systems, Phys. Rev. E 51 (2) (1995) 980–994.
[22] Y. Soen, N. Cohen, D. Lipson, E. Braun, Emergence of spontaneous rhythm disorders in self-assembled networks of heart cells, Phys. Rev. Lett. 82 (17) (1999) 3556–3559.
[23] A. Stefaski, P. Perlikowski, T. Kapitaniak, Ragged synchronizability of coupled oscillators, Phys. Rev. E 75 (2007).
[24] B. Van der Pol, Theory of the amplitude of free forced triod vibration, Radio Rev. 1 (1920) 701–710.
[25] B. Van der Pol, Forced oscillations in a circuit with non-linear resistance (reception with reactive triode), The London, Edinburgh, and Dublin Philosophical Magazine and Journal of Science Ser. 7 3 (1927) 65–80.
[26] B. Van der Pol, J. Van der Mark, Frequency demultiplication, Nature 120 (1927) 363–364.
[27] D.J. Watts, S.H. Strogatz, Collective dynamics of 'small-world' networks, Nature 393 (1998) 440–442.
[28] H.G. Winful, L. Rahman, Synchronized chaos and spatiotemporal chaos in arrays of coupled lasers, Phys. Rev. Lett. 65 (13) (1990) 1575–1578.
[29] C.W. Wu, L. Chua, A unified framework for synchronization and control of dynamical systems, Int. J. Bifurcation Chaos (IJBC) 4 (1994) 979–998.
[30] T. Yamada, H. Fujisaka, Stability theory of synchronized motion in coupled-oscillator systems. II—the mapping approach, Prog. Theor. Phys. 70 (1983).
[31] S. Yanchuk, Yu. Maistrenko, E. Mosekilde, Partial synchronization and clustering in a system of diffusively coupled chaotic oscillators, Math. Comput. Simul. 54 (2000) 491–508.
[32] S. Yanchuk, K.R. Schneider, L. Recke, Dynamics of two mutually coupled semiconductor lasers: instantaneous coupling limit, Phys. Rev. E 69 (5) (2004) 056221.

Please cite this article as: P. Perlikowski, et al., Discontinuous synchrony in an array of Van der Pol oscillators, Int. J. Non-Linear Mech. (2010), doi:10.1016/j.ijnonlinmec.2010.01.010